On the Indentation of a Chemically-treated Polymeric Membrane

A. P. S. Selvadurai[1], **and Q. Yu**[2]

Abstract: A characteristic feature of a polymeric material such as PVC is its hyperelasticity or the ability to experience large strains prior to failure. The exposure of PVC to chemicals such as acetone and ethanol results in embrittlement or the loss of the hyperelasticity property. In this paper, we examine the mechanical behaviour of a PVC membrane that has been exposed to ethanol. Due to leaching of the plasticizer, the constitutive response of the PVC changes from a hyperelastic material to a hardened material that displays dominant yield behaviour and particularly one that is capable of experiencing post-yield large strains and strain-rate effects. A constitutive model is developed to describe the mechanical behaviour of the PVC subjected to ethanol exposure. This constitutive model is implemented in a computational code to examine the problem of the mechanical behaviour of a chemically-treated membrane that is fixed along a circular boundary and loaded by a rigid spherical indentor. Both axisymmetric and asymmetric off-axis indentation tests are performed on the chemically-treated PVC. The load-displacement responses of the indentor as well as the profiles of the chemically-treated PVC membrane during indentation are used to assess the predictive capabilities of the constitutive model.

keyword: Chemical exposure, membrane indentation, PVC membranes, hyperelasticity, strain-rate effects, experimental modelling

1 Introduction

Over the past three decades, geosynthetics or polymeric membranes have been extensively used as components of engineered barriers constructed to prevent the migration of contaminants and other hazardous substances from waste disposal sites associated with landfill, mine wastes and residues derived from energy resources exploration (Koerner, 1994; Qian et al., 2002). Engineering experiences with geosynthetic membrane barriers is relatively recent and the reliability of the PVC and other geosynthetic materials under adverse conditions is not well understood. PVC membranes used as components of engineered barrier schemes can be subjected to a variety of mechanical, environmental and chemical loadings, including surcharge loads of accumulating landfill or mine waste, pressures generated by entrapped gases due to failure of venting systems, solar radiation, low temperatures of cold climates, and temperatures generated by exothermic processes in retained landfill. Haxo and Haxo (1989) cite several examples where such actions have been observed. The overall effect of these processes is to influence the durability of the PVC material and to severely reduce its effective life (Madorsky, 1964; Khalifa *et al*, 1979; Bacaloglu and Fisch, 1995; Cazzuffi et al., 1995). The alteration in the durability can manifest in various forms and the focus of this paper relates to the assessment of embrittlement that is observed during the loss of plasticizer, which provides the PVC with the capacity for large deformations. Experiments conducted by Haedrich (1995), Contamin and Debeauvais (1998), Bishop et al. (2000), Shin et al. (2002), and Yu and Selvadurai (2005) indicate that exposure of PVC materials to commonly occurring chemicals, including ethanol and acetone, leads to the leaching of plasticizer from PVC, resulting in a substantial reduction in the flexibility of the material. When flexibility reductions occur in a component of a barrier that is intended to sustain large strains, the resulting property changes can affect the integrity of the entire engineered barrier system. The loss of plasticizer from a PVC due to exposure to chemicals such as ethanol has been documented by Messadi et al. (1981), Messadi and Vergnaud (1982) and Yu and Selvadurai (2005). The magnitude and rate of the loss of plasticizer are generally related to the concentration of the chemical that is in contact with the PVC. In an engineered barrier that contains

---

[1] Corresponding author. William Scott Professor and James McGill Professor. Department of Civil Engineering and Applied Mechanics, McGill University, 817 Sherbrooke Street West, Montreal, QC, Canada H3A 2K6 (E-mail: patrick.selvadurai@mcgill.ca). Tel: +1 514 398 6672; fax: +1 514 398 7361

[2] Doctoral student

Table 1 : The value of $R_{O/Cl}$ for PVC membranes exposed to ethanol, water and ethanol-water mixtures

Specimen	$R_{O/Cl}$
PVC membrane as supplied	6.47%
18-*month* water exposure	5.55%
16-*month* 50% ethanol exposure	5.44%
2-*month* pure ethanol exposure	5.33%
5-*month* pure ethanol exposure	5.20%

several components including clays and geosynthetics in sequence, the clay barriers are expected to act as a *buffer* that will minimize the level of concentration of the retained chemicals that will come into direct contact with the PVC. In situations where exothermic reactions and ground freezing can induce desiccation cracking of clay liners, its effectiveness as a buffering barrier can be lost and the retained chemical can come into direct contact with the geosynthetic. Figure 1 illustrates the continued alteration in the mechanical behaviour of a PVC material that was subjected to periods of exposure to pure ethanol, in an immersion test. The constitutive response of the PVC changes from a hyperelastic to a hardened material that displays a dominant yield behaviour.

The work of Pita et al. (2002) shows that a monotonically increasing relationship exists between stress and strain for a plasticized PVC with a high plasticizer content. When the plasticizer content is lowered, a stress-strain response with a distinct yield-type phenomenon is observed (Figure 2). We can infer that the most likely factor contributing to embrittlement phenomena in a plasticized PVC is the loss of the plasticizer. An X-ray fluorescence technique can also be used to determine the plasticizer content of the chemically-treated PVC membrane exposed to pure ethanol for different durations. The PVC used in this research has been originally plasticized with 25%-35% by weight of a phthalate plasticizer (Diebel, 2002). The plasticizer content can then be measured through the weight ratio $R_{O/Cl}$, which corresponds to the oxygen element and the chloride element. Although these measurements give only surface alterations in the plasticizer content, tests conducted on samples of the PVC of a thickness of 0.5*mm* show a continued reduction in the ratio $R_{O/Cl}$ with the duration of exposure (Table 1), which again points to the loss of plasticizer as a possible factor contributing to the alteration in the mechanical behaviour.

The purpose of this research is to gain a better understanding of the mechanical behaviour of the PVC material during its exposure to pure ethanol over a period up to 9 *months*. The experimental research program commences with the uniaxial testing of the membrane material, which is used to develop constitutive models for PVC both in its untreated and treated states. The details of the constitutive model development are presented elsewhere (Selvadurai and Yu, 2005a). In this paper, the focus is on the application of the constitutive relationships developed to the computational modelling of the static response of a circular membrane that is fixed along a circular boundary and subjected to either axisymmetric or asymmetric off-axis indentation through a rigid spherical indentor (Figure 3). The topics of indentation and inflation of membranes have been extensively researched particularly in connection with the study of the mechanics of the rubber-like materials. A comprehensive account of developments in this area is given by Selvadurai and Yu (2005b). The constitutive model for the PVC subjected to ethanol exposure used in this paper takes into consideration effects of large strains, presence of a distinct yield phenomenon in the stress-strain response, strain-rate effects and the development of irreversible deformations during a loading cycle. The indentation problem is intended to simulate situations where the geosynthetic membrane can be subjected to localized loading during the operation of a waste disposal facility. The investigations also focus on both asymmetric and off-axis indentation of the treated membrane, which are intended to assess the predictive capabilities of computational approaches that also account for the influence of friction generated between the chemically-treated membrane and the spherical indentor. The frictional contact characteristics determined via separate experiments, are implemented in the computational modelling.

2 Constitutive modelling

The mechanical behaviour of hyperelastic pure rubber-like materials is characterized by imperceptible permanent deformations that accompany their responses under quasi-static load cycling. The modelling of the mechanical behaviour of such materials represents an important development in modern non-linear continuum mechanics and accounts of the constitutive model developments associated with rubber-like hyperelastic materials both from the kinetic theories and phenomenological

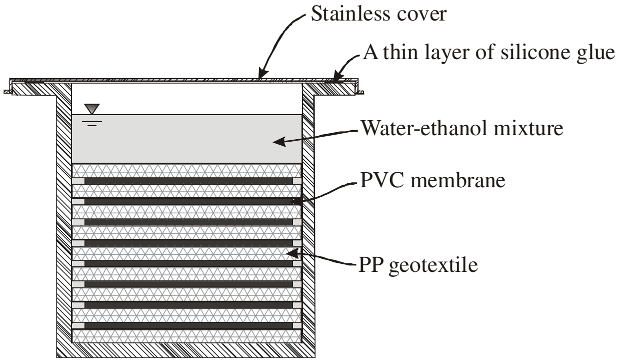

(a) Immersion test for PVC membrane subjected to chemical exposure

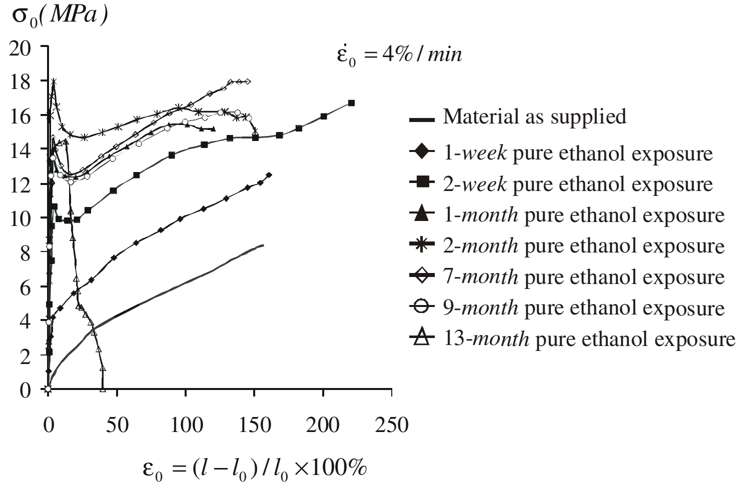

(b) Uniaixial behaviour of PVC membrane exposed to pure ethanol

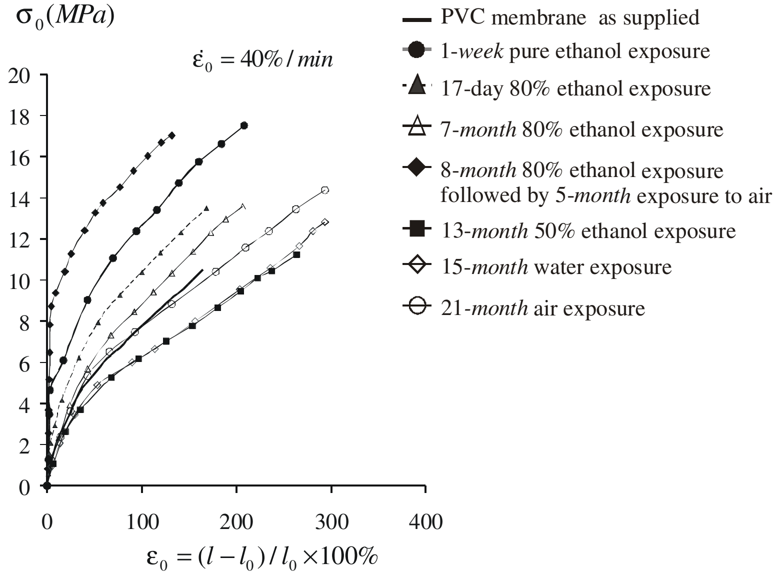

(c) Response of PVC membrane exposure to concentrations of ethanol

Figure 1 : Uniaxial behaviour of a chemically-treated PVC membrane

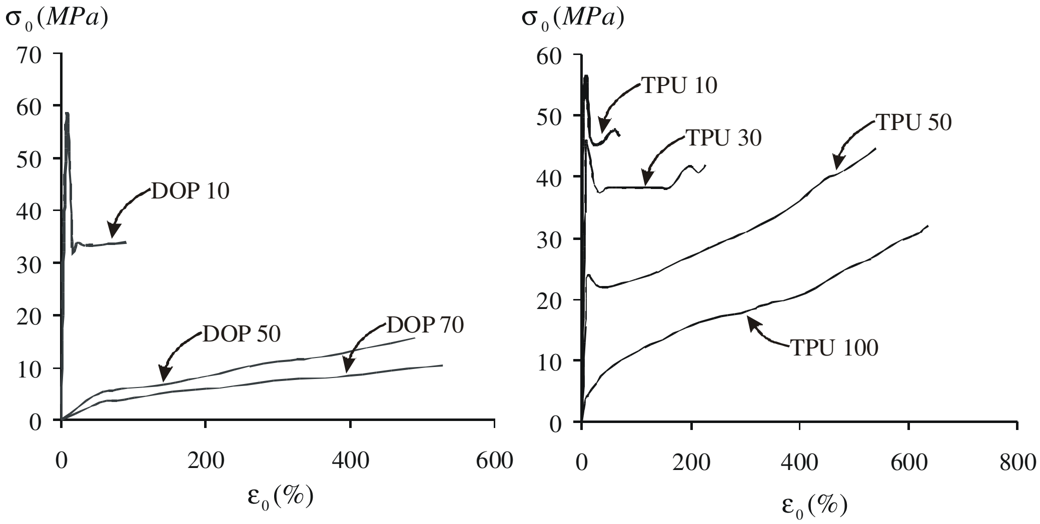

(a) Plasticized with DOP (in *phr*) (b) Plasticized with TPU (in *phr*)

Figure 2 : Stress-strain curve of plasticized PVC with different amounts of plasticizer (after Pita et al., 2002)

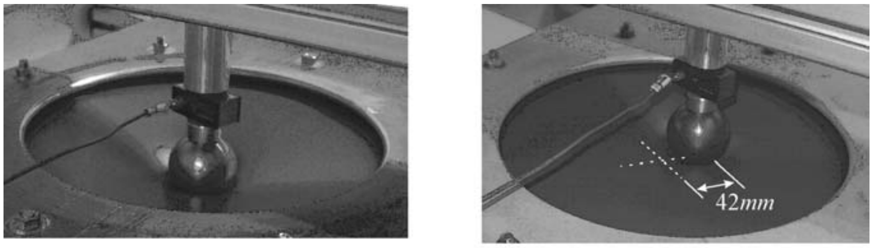

(a) Axisymmetric indentation (b) Asymmetric indentation

Figure 3 : Indentation of a chemically-treated PVC membrane

points of view are given by Treloar (1943, 1975), Rivlin (1948, 1960), Flory (1969), Green and Adkins (1970), Spencer (1970), Edwards (1971), Ogden (1984), and Selvadurai (2002), Rubber-like hyperelastic materials can exhibit path-dependency and hysteretic effects in their stress-strain behaviour that are attributed to phenomena such as the “Mullins effect” (Mullins, 1947, 1969; Farris, 1971; Beatty, 1987; Dorfmann and Ogden, 2005). Septanika and Ernst (1998a,b) have applied the network alteration theory to account for the time-dependent behaviour of a rubber-like material. In the present paper, we examine the constitutive response of a chemically-treated PVC that displays irreversible phenomena that are distinctly different from those observed in connection with the Mullins effect and discussed in the developments presented by Septanika and Ernst (1998a,b). The exposure of a plasticized PVC to chemicals such as ethanol and acetone results in the gradual removal of the plasticizer from the PVC. The removal of the plasticizer gives rise to drastic changes in the mechanical behaviour of the original material. The most noticeable of these is the loss of hyperelasticity or embrittlement. Furthermore, the chemically-treated and plasticizer-depleted material also develops a distinct yield point in the stress-strain response. The chemically-treated material also displays sensitivity to strain-rate effects (see also Arruda et al., 1995; Qi and Boyce, 2004). The typical stress-strain responses of the PVC subjected to ethanol exposure are presented by Yu and Selvadurai (2005) and details associated with the constitutive model development are described by Selvadurai and Yu (2005a). It can be shown that the development of the constitutive model is compatible with thermodynamical constraints that should accompany constitutive model development (Selvadurai and Yu, 2005a). For completeness, the salient features of the constitutive model and its ability to duplicate and predict experimental results derived from uniaxial tests are summarized.

To describe the deformations, we consider a generic particle, the position of which in the deformed configuration is denoted by x_i $(i = 1,2,3)$; and its coordinates in the reference configuration are denoted by X_A $(A = 1,2,3)$. The deformation gradient tensor is given by

$$\boldsymbol{F} = \partial x_i / \partial X_A \tag{1}$$

Following Kröner (1960) and Lee (1969) (see also Pipkin and Rivlin; 1970; Owen, 1970; Clifton, 1972; Boyce et al., 1988a,b; Pereda et al., 1993; Ahzi et al., 2003; Lubarda, 2004; Gurtin and Anand, 2005), we assume that the total deformation gradient tensor $\boldsymbol{F}$ can be decomposed into its elastic (e) and irreversible (u) components in a multiplicative manner; i.e.

$$\boldsymbol{F} = \boldsymbol{F}^e \boldsymbol{F}^u \tag{2}$$

Strain tensors in terms of $\boldsymbol{B}^e$ and $\boldsymbol{B}^u$are defined by

$$\boldsymbol{B}^e = \boldsymbol{F}^e (\boldsymbol{F}^e)^T; \quad \boldsymbol{B}^u = \boldsymbol{F}^u (\boldsymbol{F}^u)^T \tag{3}$$

and the strain-rates are defined by (Malvern, 1969; Spencer, 2004)

$$\begin{aligned} \boldsymbol{L} &= \dot{\boldsymbol{F}} \boldsymbol{F}^{-1} = \boldsymbol{D} + \boldsymbol{W} \\ &= \dot{\boldsymbol{F}}^e (\boldsymbol{F}^e)^{-1} + \boldsymbol{F}^e \left[\dot{\boldsymbol{F}}^u (\boldsymbol{F}^u)^{-1} \right] (\boldsymbol{F}^e)^{-1} \\ \boldsymbol{L}^u &= \dot{\boldsymbol{F}}^u (\boldsymbol{F}^u)^{-1} \\ \boldsymbol{D}^u &= \frac{1}{2} \left[\boldsymbol{L}^u + (\boldsymbol{L}^u)^T \right] \end{aligned} \tag{4}$$

The invariants of $\boldsymbol{B}^e$, $\boldsymbol{B}^u$ are

$$\begin{aligned} I_1^h &= (\lambda_1^h)^2 + (\lambda_2^h)^2 + (\lambda_3^h)^2 \,; \\ I_2^h &= \frac{1}{(\lambda_1^h)^2} + \frac{1}{(\lambda_2^h)^2} + \frac{1}{(\lambda_3^h)^2} \,; \ (h = e, u) \\ I_3^h &= \lambda_1^h \lambda_2^h \lambda_3^h \,; \end{aligned} \tag{5}$$

and λ_i^e and $\lambda_i^u \quad (i = 1,2,3)$ are respectively the principal stretches of the elastic and irreversible components. The constitutive model for the PVC material selected here has a generic form, with components as shown in Figure 4. The calibration of the results of experimental investigations with a wider class of internal energy functions indicates that at moderately large strains, the loading behaviour of the untreated PVC membrane material can be adequately characterized by an internal energy function of the Mooney-Rivlin type (Mooney, 1940; Rivlin, 1948). Also, the condition of material incompressibility is implicit in the Mooney-Rivlin form of an internal energy function. Experimental evidence associated with the current research indicates that this assumption is nearly satisfied by the PVC material maintaining a value of $I_3 \in [0.982, 0.993]$.

To maintain consistency with developments applicable to the modelling of the untreated PVC and to account for moderately large strains that can occur in the chemically-treated PVC, we assume that the component C of the model (Figure 4) applicable to the treated PVC can be represented by an internal energy function of Mooney-Rivlin type. The component C is sufficient to characterize the constitutive behaviour of the PVC material during *monotonic loading without unloading*. In this case, irreversible effects are not accounted for and the total deformation gradient and $\boldsymbol{F}$ is interpreted as the elastic deformation gradient $\boldsymbol{F}^e$. We assume that the stress $\boldsymbol{T}_C$ associated with the model C, which is the total Cauchy stress $\boldsymbol{T}$ for the treated PVC material, is an isotropic function of elastic strain tensor $\boldsymbol{B}^e$. Furthermore, we restrict attention to chemically-treated materials that display incompressible behaviour in their mechanical response associated with the component C. With these restrictions, the constitutive equation that governs the element C can be written as

$$\begin{aligned} \boldsymbol{T} &= \boldsymbol{T}_C = -\tilde{p}^e \boldsymbol{I} + \psi_1^e \boldsymbol{B}^e + \psi_2^e (\boldsymbol{B}^e)^2 \\ \psi_1^e &= 2 \left(\frac{\partial W^e}{\partial I_1^e} + I_1^e \frac{\partial W^e}{\partial I_2^e} \right) \\ \psi_2^e &= -2 \frac{\partial W^e}{\partial I_2^e} \end{aligned} \tag{6}$$

where $\tilde{p}^e$ is a scalar pressure. Influence of strain-rate effects on the hyperelastic behaviour has been discussed by a number of authors including Sweeney and Ward (1995) and Matthews *et al.* (1997). Following the approach proposed by Sweeney and Ward (1995) to account for the influence of strain-rate effects on the internal energy function, we adopt the following form of an internal energy function for the chemically-treated PVC material:

$$W^e(I_1^e, I_2^e) = C_1'(I_1^e - 3) \tag{7}$$

where

$$C_1' = C_1 + \begin{cases} \kappa_1 \ln(|\dot{\gamma}_0| / \dot{\gamma}_c) & (|\dot{\gamma}_0| \geq \dot{\gamma}_c) \\ 0 & (|\dot{\gamma}_0| < \dot{\gamma}_c) \end{cases} \tag{8}$$

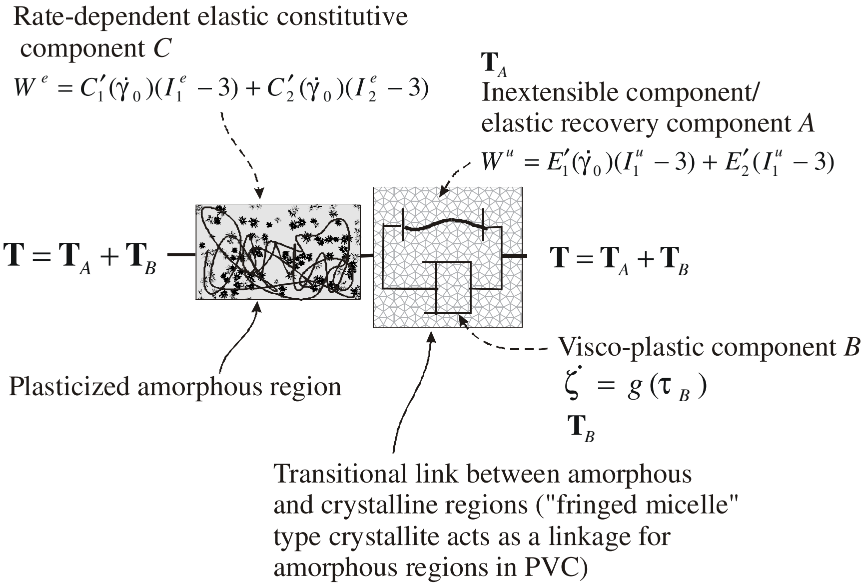

Figure 4 : Schematic representation of the constitutive components

A rationale for incorporating the dependency of W on strain-rate effects is also presented by Selvadurai and Yu (2005a). Also, $\dot\gamma_0$ is a generalized form of a combined stretch-rate that depends only on the three principal stretches λ_i $(i = 1,2,3)$ according to

$$\dot\gamma_0 = \frac{d\gamma_0}{dt}; \qquad \gamma_0 = \left[(\bar\lambda_1 - 1)^{\frac{1}{\alpha}} + (\bar\lambda_2 - 1)^{\frac{1}{\alpha}} + (\bar\lambda_3 - 1)^{\frac{1}{\alpha}}\right]^{\alpha} \tag{9}$$

where, $\bar\lambda_i$ $(i = 1,2,3)$ have a conditional dependence on the total principal stretches λ_i, to take into consideration either the *loading* or the *unloading* response: i.e.

$$\bar\lambda_i = \begin{cases} \lambda_i; & (\lambda_i \geq 1) \quad i = (1,2,3) \\ 1; & (\lambda_i < 1) \quad i = (1,2,3) \end{cases} \tag{10}$$

and α is a material parameter that accounts for states of combined stretch. When the test specimen is subjected to a uniaxial stretch, the principal stretches in the lateral directions are less than unity and the definition of γ_0 reduces to that of the uniaxial strain ε_0. In (8), C_1' is the modified Mooney-Rivlin parameter; κ_1 is the parameter that defines the strain-rate sensitivity and $\dot\gamma_c$ is defined as the *rate-independent threshold strain-rate*. At loading rates $|\dot\gamma_0| \leq \dot\gamma_c$, the strain-rate effects in C_1' are disregarded.

The chemically-treated PVC materials subjected to levels of strain beyond the yield point will exhibit permanent strains. A possible way to model this response is to incorporate an additional elastic-visco-plastic model that is characterized by an elastic recovery component A in parallel with a visco-plastic component B, which should be added in series to the component C (Figure 4). Since the component A accounts for elastic unloading at moderately large strains, we assume that this behaviour can be represented by a constitutive relationship of a form applicable to incompressible materials:

$$\boldsymbol{T}_A = -\tilde p^u \boldsymbol{I} + \psi_1^u \boldsymbol{B}^u + \psi_2^u (\boldsymbol{B}^u)^2; \quad \psi_1^u = 2\left(\frac{\partial W^u}{\partial I_1^u} + I_1^u \frac{\partial W^u}{\partial I_2^u}\right); \quad \psi_2^u = -2\frac{\partial W^u}{\partial I_2^u} \tag{11}$$

where $\tilde p^u$ is a scalar pressure and

$$W^u(I_1^u, I_2^u) = E_1'(I_1^u - 3) + E_2'(I_2^u - 3) \tag{12}$$

The work of Rittel (1999, 2000) indicates that the plastic energy dissipation of a glassy polymer prior to yield is usually negligible. To account for such a response, in (12), E_1' is subject to the conditional constraint:

$$E_1' = \begin{cases} \to \infty; & (\dot\gamma_0 \geq -\dot\gamma_c^y \ \text{ and } \ \gamma_0 \leq \zeta_y) \\ E_y'; & (\dot\gamma_0 \geq -\dot\gamma_c^y \ \text{ and } \ \gamma_0 > \zeta_y) \\ 0; & (\dot\gamma_0 < -\dot\gamma_c^y) \end{cases} \tag{13}$$

where ζ_y is the yield strain of the chemically-treated PVC material and E_2' is a constant. The particular representation for E_1' given by (13) can take into account the fully elastic behaviour of the chemically-treated PVC prior to yield at a loading rate $\dot{\gamma}_0 \geq -\dot{\gamma}_c^v$, where the visco-plastic deformation is restricted due to the infinite value of E_1' associated with the conditional constraint. A non-zero finite value of E_1' beyond the yield point, however, results in the development of visco-plastic deformation, which leads to a softening behaviour of the material and subsequent hardening behaviour in the large strain range (e.g. $\varepsilon_0 = 100\% \sim 150\%$). Upon unloading (i.e. $\dot{\gamma}_0 < -\dot{\gamma}_c^v$), the visco-plastic deformation is fully activated due to the zero value of E_1', which results in irreversible visco-plastic permanent strains. It is also possible to interpret the presence of a high modulus prior to yield in terms of the deformability of a transitional link between the amorphous regions and the crystalline regions. The inextensible transitional link can only take incremental loading, but zero incremental unloading. The papers by Boue et al. (1988) and Jones and Marques (1990) investigate the concepts underlying the behaviour of an inextensible strand connecting two neighboring junctions in a polymeric material. The existence of the "fringed micelle" type crystallite acting as a linkage for the amorphous network of PVC material was confirmed in the experimental and analytical work of Aiken et al. (1947), Alfrey et al. (1949a) and Alfrey et al. (1949b). In the work by Qi and Boyce (2005), which deals with the mechanics of a polymeric material containing hard and soft segments, the hard segments are also considered to act as a physical crosslink for the soft segments, a role similar to that of a crystallite region connecting the amorphous regions. In particular, Alfrey et al. (1949b) found that the crystallites presented an oriented structure after a pre-stretch history. Of related interest is the study by Ahzi et al. (2003), which deals with the activity of strain-induced crystallization. We therefore assume that due to oriented alignment between the amorphous network and the crystallite, the region at their connection cannot sustain any unloading immediately followed by a monotonic loading. The transitional link also has limited deformability. At $\varepsilon_0 = \gamma_0 = \zeta_y$, it breaks resulting in material softening and subsequent hardening at large strains (e.g. $\varepsilon_0 = 100\% \sim 150\%$). The possible influence of rate-dependency of E_y' in (13) is accounted for through the relationship

$$E_y' = E_y + \begin{cases} \kappa_y \ln(|\dot{\gamma}_0|/\dot{\gamma}_c^v); & (|\dot{\gamma}_0| \geq \dot{\gamma}_c^v) \\ 0; & (|\dot{\gamma}_0| < \dot{\gamma}_c^v) \end{cases} \tag{14}$$

where κ_y is the rate-sensitivity and E_y is the *rate-independent hardening modulus*.

The Cauchy stress tensor $\boldsymbol{T}_B$ in component B of the phenomenological model shown in Figure 4 is defined in terms of the irreversible finite strain-rate tensor $\boldsymbol{D}^u$, which is assumed to be related to the deviatoric component of the normalized effective stress tensor $\boldsymbol{N}_B$ (see also Boyce et al., 1988a, b; Gurtin and Anand, 2005). Visco-plastic effects, in the component B, are modelled through a relationship of the form

$$\begin{gathered} \boldsymbol{D}^u = \dot{\zeta}\boldsymbol{N}_B; \quad \boldsymbol{N}_B = \frac{3}{2\tau_B}\boldsymbol{T}'_B; \\ \tau_B = \left\{ \frac{3}{2} tr\left[\left(\boldsymbol{T}'_e\right)^2 \right] \right\}^{1/2} \end{gathered} \tag{15}$$

where $\boldsymbol{T}'_B$ is the deviatoric component of $\boldsymbol{T}_B$ and τ_B is an effective stress applicable to visco-plastic phenomena as depicted in Figure 4. Also, in (15) the visco-plastic strain-rate $\dot{\zeta}$ is generally assumed to be a function of τ_B and the strain-rate $\dot{\gamma}_0$, i.e.

$$\dot{\zeta} = \left(\frac{\tau_B}{q}\right)^{1-s} |\dot{\gamma}_0| \begin{cases} \dfrac{1}{(|\dot{\gamma}_0|/\dot{\gamma}_c^v)^s}; & (|\dot{\gamma}_0| \geq \dot{\gamma}_c^v) \\ 1; & (|\dot{\gamma}_0| < \dot{\gamma}_c^v) \end{cases} \tag{16}$$

In (16), $s \in [0,\ 1]$ is the *viscous sensitivity* to the strain-rate effect. At loading rates lower than the critical value (i.e. $|\dot{\gamma}_0| \leq \dot{\gamma}_c^v$), the dependency of $\dot{\zeta}$ on the strain-rate ratio $\dot{\gamma}_0/\dot{\gamma}_c^v$ is neglected. At these loading rates and at the start of yield, $\tau_B = q$ and (16) reduces to $d\zeta \approx d\gamma_0$ (or $d\zeta \approx d\varepsilon_0$ in a unaixial test). The contribution of model C to the overall stress-strain response in uniaxial loading is therefore marginal. The parameter q can then be interpreted as a *static yielding stress* of the material, giving rise to $q = 6C_1\zeta_y$.

Following Boyce et al. (1988a, b), the stress states in the elastic recovery responses A (denoted by $\boldsymbol{T}_A$) and the visco-plastic responses B (denoted by $\boldsymbol{T}_B$) are added to generate the Cauchy stress $\boldsymbol{T}$: i.e.

$$\boldsymbol{T} = \boldsymbol{T}_C = \boldsymbol{T}_A + \boldsymbol{T}_B \tag{17}$$

In summary, a generalized form of a constitutive model capable of describing yield-type phenomena, large strain hyperelastic behaviour, strain-rate effects and moderately large irreversible plastic strains has been adopted to describe the mechanical behaviour of the chemically-treated PVC material. The mechanical response, however, has to distinguish between loading and unloading behaviour through a selective definition of the elasticity parameters of the elastic recovery component. The response of this component also takes into account the yield-type phenomena. Prior to yield, the visco-plastic deformation is suppressed and beyond the yield point the visco-plastic effects that account for further softening and hardening behaviour are activated. Upon unloading, the visco-plastic component is fully activated and unloading behaviour is accompanied by irreversible deformations. Tables 2 gives a summary of the equations used for describing the general form of the constitutive model for the chemically-treated PVC during both loading and unloading stress histories.

Table 3 gives a summary of the material parameters that are used to describe the constitutive models for the chemically-treated PVC at various durations of exposure to pure ethanol. It is noted that there is a set of material parameters that is essentially uninfluenced by the duration of chemical exposure; these are $\zeta_y = 2.8\%$; $\dot{\gamma}_c \approx 5.67 \times 10^{-7}\text{sec}^{-1}$; $\dot{\gamma}_c^v \approx 3.2 \times 10^{-10}\,\text{sec}^{-1}$; $E_2' \approx 1.2MPa$. The model representations of the experimental data conducted up to failure at loading rates $\dot{\varepsilon}_0 = 4\%/\text{min}$ and $\dot{\varepsilon}_0 = 40\%/\text{min}$ for samples subjected to different durations of exposure are presented in Figure 5.

The results of the uniaxial tests are insufficient to determine the parameter α that accounts for combined stretch. The effects of this parameter become appreciable when the PVC specimen experiences bi-axial stretching. The biaxial stretching of the PVC specimen was achieved by stretching a square specimen fixed along oblique directions inclined at 45° to the axis of loading (see Figure 6a). Fixity was enforced at the boundaries of the tested specimen using a pair of aluminum grips. (At the time of conducting this test, the specimens subjected to 9 *months* of exposure to pure ethanol had all been used up in the uniaxial and indentation tests.) The material parameter α was therefore determined by conducting tests on samples of the PVC that were subjected to 5 *months* of exposure to ethanol followed by 7 *months* of exposure to air. The experiments were first conducted on samples of the untreated PVC. The observations of the distortion of a grid marked on the test specimen indicate that regions of the test specimen do experience biaxial effects at large deformations. The experimental program also examined the response of a PVC specimen subjected to 5 *months* of exposure to pure ethanol followed by a 7-*month* exposure to air. It was concluded that the swelling phenomenon due to the absorption of the moisture resulted in the possible "softening" of the PVC specimen at longer durations of exposure to pure ethanol (see Figure 1b). The exposure to air then leads to the removal of the moisture and ethanol within the chemically-treated PVC. Therefore the response of a chemically-treated specimen subjected to prolonged exposure to air results in a stiffer mechanical response (Figure 6b) when compared to the stress-strain responses of the chemically-treated PVC in the absence of exposure to air (Figure 1b). The constitutive model proposed in the paper together with the set of material parameters shown in Table 3 were used to examine the computational responses of the uniaxial test with oblique fixity. Since the plasticizer loss appears to stabilize after 5 *months* of exposure (Table 1), it may be concluded that the material parameter α is relatively uninfluenced by the duration of chemical exposure. The material parameter $\alpha \approx 3$ is therefore considered to be applicable to PVC specimens exposed to pure ethanol for a period of 9 *months*. The particular value of $\alpha \approx 3$ is possibly indicative of equal contributions from the three principal stretch directions of the polymeric material in the definition of $\dot{\gamma}_0$ in (9).

3 The indentation of the chemically-treated membrane

The membrane indentation test facility shown in Figure 7a is designed to apply a controlled movement (Δ) to a rigid spherical indentor (of diameter 50.8*mm*) that interacts with a membrane fixed along a circular boundary. All tests were conducted on PVC specimens that were exposed to ethanol for a period of 9 *months*. The rate of indentation $\dot{\Delta}$ is set constant during a test. The test facility has provisions for securing a plane membrane specimen in a fixed condition along a circular boundary of diameter 250*mm* (see Figure 7b). The fixed boundary condition is achieved by clamping of the PVC specimen between two aluminum plates (5*mm* in thickness) using eight 4*mm* screws. To reduce the possibility of slippage at the clamped boundary, a rubber sheet of thickness

Table 2 : Constitutive equations used for modelling chemically-treated PVC material exposed to pure ethanol

Components	Deformation gradient	Component A ($\boldsymbol{T}_A$)	Component B ($\boldsymbol{T}_B$)	Component C ($\boldsymbol{T}_C$)
Loading prior to yield	$\boldsymbol{F} = \boldsymbol{F}^e$	Deformation restricted	Deformation restricted	Eq. (2.6), (2.7), (2.8),(2.9), (2.10)
Loading beyond the yield point	$\boldsymbol{F} = \boldsymbol{F}^e\boldsymbol{F}^u$	Eq. (2.11), (2.12) with $E_1' = E_y'$, (2.14)	Eq. (2.15), (2.16)	
Unloading	$\boldsymbol{F} = \boldsymbol{F}^e\boldsymbol{F}^u$	Eq. (2.11), (2.12) with $E_1' = 0$, (2.14)	Eq. (2.15), (2.16)	

Table 3 : Material parameters of the treated PVC at different durations of pure ethanol exposure

Exposure period to pure ethanol	Parameters that are influenced by exposure duration						Parameters that are uninfluenced by duration of chemical exposure
	Component A		Component B		Component C		
	$E_y(MPa)$	κ_y	s	$q = 6C_1\zeta_y$ (MPa)	$C_1(MPa)$	κ_1	$\zeta_y \approx 2.8\%$; $\dot{\gamma}_c \approx 5.67 \times 10^{-7}\text{sec}^{-1}$; $\dot{\gamma}_c^v \approx 3.2 \times 10^{-10}\,\text{sec}^{-1}$; $E_2' \approx 1.2MPa$; $\alpha \approx 3^*$
1 *week*	3.4	0.13	0.06	2	11.9	2.0	
2 *months*	2.88	0.087	0.115	2.3	13.7	13.0	
7 *months*	1.13	0.13	0.10	2.4	14.3	12.06	
9 *months*	1.90	0.087	0.09	2.6	15.0	9.0	
5 *months* followed by 7-*month* air exposure	4.13	0.87	0.11	4.2	25.0	19.0	

$*$ The effects of the parameter are unappreciable in uniaxial loading cases

3*mm* with an opening of diameter 250*mm* was bonded to the PVC specimen, using a non-reactive instant adhesive. During axisymmetric indentation, the contacts were initiated at the center of the circular membrane (Figure 3a). The indentation response was prescribed through the application of the indentation displacement in an incremental manner up to a maximum displacement of $\Delta_{\max} = 50.8\,mm$.

During axisymmetric loading of the chemically-treated PVC, the ratio of the maximum indentor displacement to the membrane diameter reached approximately 0.20. This corresponds to a maximum strain of 20% at the line of separation at the contact. The load (P) indentor displacement (Δ) response during axisymmetric indentation and the displaced profiles of the membrane are shown in Figure 8a. The results show a good repeatability between the sets of experiments. The visual images of the deflected shapes were recorded using a high precision (5 Mega pixels) digital camera, which was positioned 1.5*m* from the test specimen. The digital camera was mounted on the test frame in such a way that the image plane was parallel to the plane of the symmetry of the indentation of the membrane. The chemically-treated PVC material exhibits pronounced irreversible deformations after a loading-unloading cycle. During asymmetric indentation, the contacts were initiated at a distance of 42*mm* from the central axis of the circular membrane (Figure 3b). The indentation responses were examined up to a maximum displacement of $\Delta_{\max} = 38.1\,mm$, which gave rise to a maximum strain of approximately 27% at the line of separation of contact. In comparison to the case of the axisymmetric indentation, larger forces are needed to induce the same indentational displacement (Figure 8b).

The frictional characteristics between the chemically-treated PVC and the brass indentor can influence the measured indentation responses. It was noted in the literature that the friction coefficient for the PVC materials varies with the plasticizer content (Masada et al., 1994).

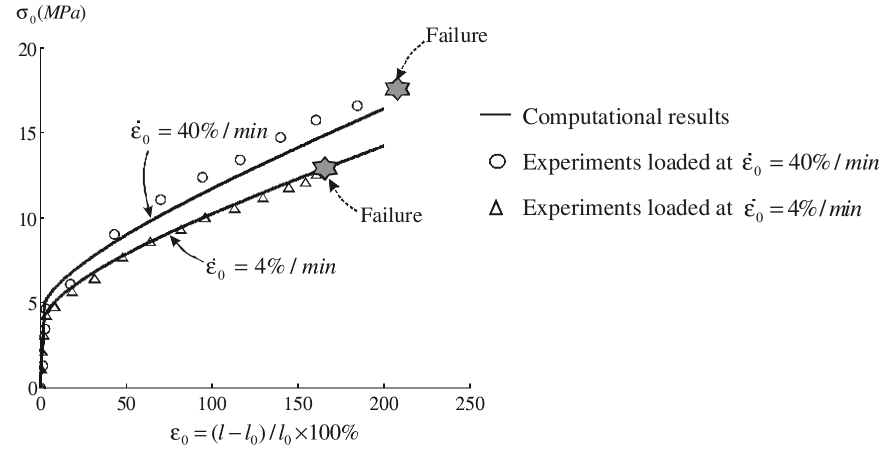

(a) 1-*week* exposure to pure ethanol

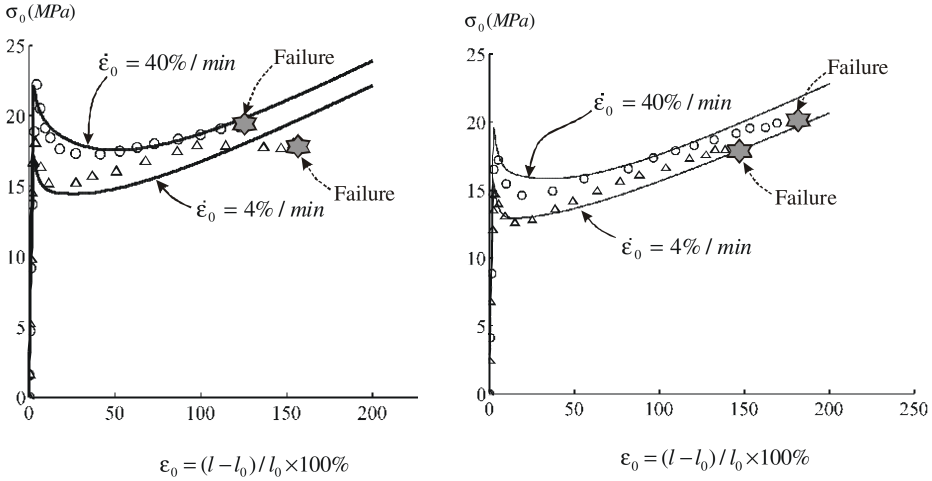

(b) 2-*month* exposure to pure ethanol (c) 7-*month* exposure to pure ethanol

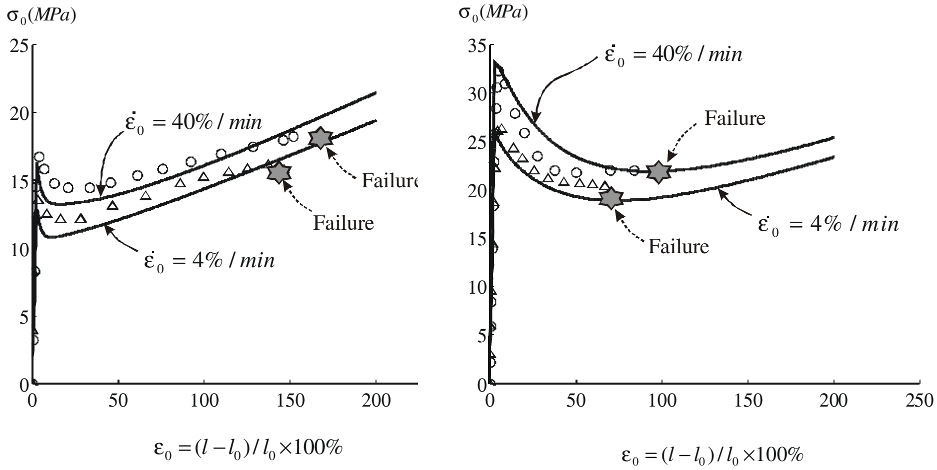

(d) 9-*month* exposure to pure ethanol (e) 5-*month* exposure to pure ethanol followed by 7-*month* exposure to air

Figure 5 : Model representations by MATLAB© software of the loading behaviour of the PVC subjected to different durations of exposure to pure ethanol

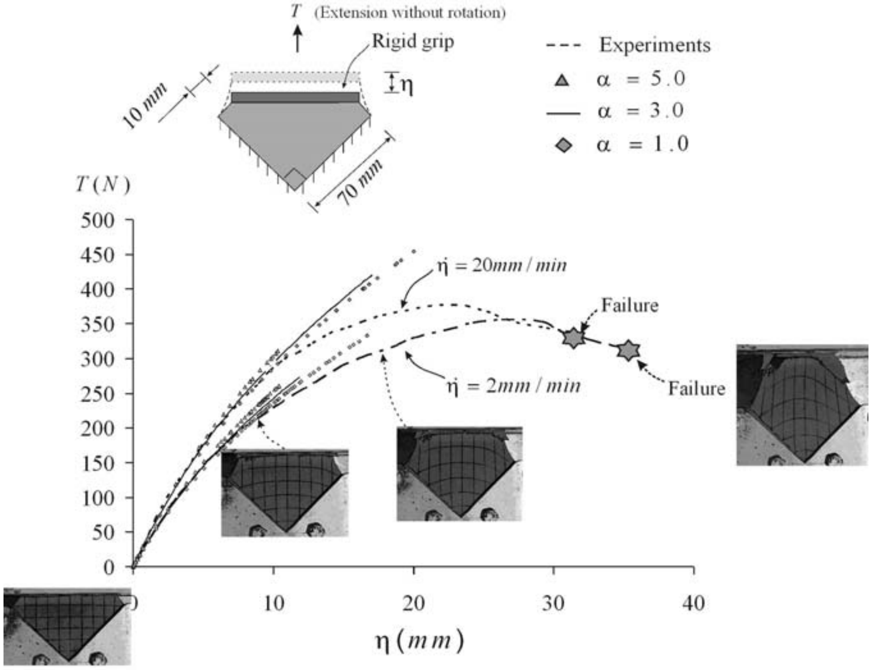

(a) Untreated PVC

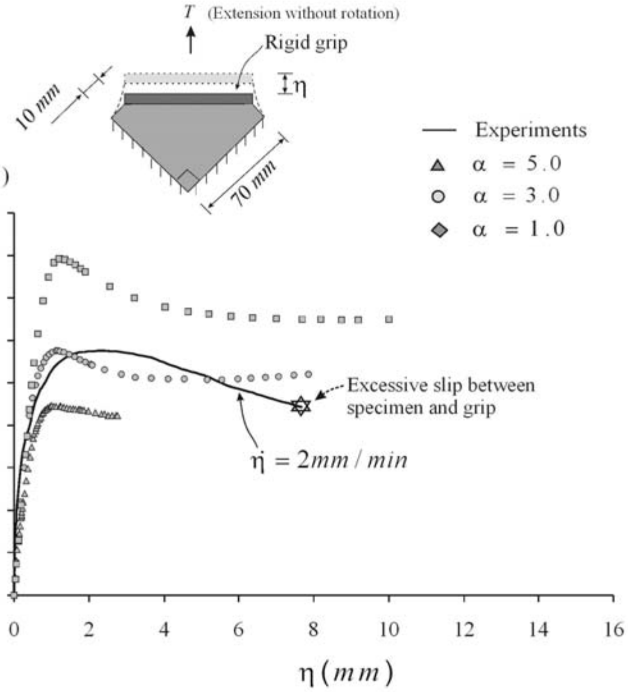

(b) PVC subjected to 5 *months* of exposure to pure ethanol followed by a 7-*month* exposure to air

Figure 6 : Experimental determination of the material parameter α

Since the chemical exposure leads to the leaching of the plasticizer from the PVC, it is necessary to conduct an independent test to estimate the frictional properties that are appropriate for the PVC exposed to pure ethanol for a 9 *month* period. During the friction experiments, a polished bronze surface (with maximum asperity difference of $0.5 \times 10^{-6} m$) measuring $127mm \times 127mm$ (see Figure 9b) is made to move with a relative displacement φ, at a controlled speed, on the surface of a chemically-treated PVC membrane that is fixed at the base (Figure 9a).

Two LVDTs that were attached to the sliding plate showed that the rotation of the moving brass plate was negligible when the membrane was bonded (using a non-reactive instant adhesive) to a fixed flat Plexiglas plate. The experiment also indicated that the normal pressure and a relative velocity between the brass surface and the PVC membrane had a negligible influence on the load-displacement behaviour. Although the indentation of the membrane gave rise to an estimated maximum normal pressure of $450kPa$, to avoid the influence of the vertical compression of the membrane during frictional test, a normal stresses σ_n as low as $6.14kPa$ was applied to the membrane using static weights. By estimating that the asymmetric indentation of the membrane can involve a maximum relative velocity of $0.5mm/\sec$ between the indentor and PVC membrane, the friction test was conducted at this displacement rate. Considering the low sliding rates, the inertial effects of the applied weight can be neglected. Figure 9c shows the variation in the applied friction force for the chemically-treated PVC with respect to the normalized relative shear displacement. For purposes of comparison, the results for frictional behaviour of the untreated PVC are also presented in Figure 9c. The difference between the static and dynamic values of friction coefficients is found to be less than the experimental error for both cases. In the experiment conducted by Pooley and Tabor (1972), these two values were also close for experiments involving contact between an untreated PVC polymer and metal surfaces. The average value of the friction coefficient during three sets of tests was estimated to be 0.08. In view of the fact that the friction was measured at a much lower normal stress than that experienced by the membrane during indentation, in the computational modelling, the value of the coefficient of friction is assigned a range of $\mu \in [0,\ 1.0]$, where the lower limit corresponds to frictionless contact between the indentor and PVC membrane and the upper limit corresponds to a coefficient of friction an order of magnitude higher than that determined from experiments.

The research program dealing with the membrane indentation problem also examined the axisymmetric indentation responses conducted on PVC samples exposed to ethanol concentrations of 50% and 80%. At these concentrations the PVC exhibited a slower rate of leaching of the plasticizer (Table 1) and generally maintained their hyperelastic large strain deformability characteristics (Figure 1c). In particular, the PVC material exposed to a 50% ethanol solution 'softened' after a prolonged exposure indicating better flexibility in resisting the localized loading compared to those exposed to pure ethanol. The possible cause of the "softening" behaviour could be attributed to the swelling of the PVC due to moisture absorption over a prolonged exposure. The membrane indentation tests conducted on the chemically-treated PVC membranes subjected to a maximum displacement of $\Delta_{\max} = 76.2mm$ gave rise to a maximum strain of 40% at the line of separation of contact. Figure 10 shows the load-indentor displacement responses during the indentation of the chemically-treated PVC membranes subjected to lower levels of ethanol concentrations. As the ethanol concentration is reduced, much lower indentational loads are required to attain the same indentational displacement.

4 Computational results

The computational modelling of the indentation of the chemically-treated PVC was performed using the general-purpose finite element code ABAQUS (ABAQUS/Standard, 2004). The nonlinear problem in the ABAQUS software is solved using a Newton-Raphson algorithm. The computational procedure used in the ABAQUS program is indicated in the flow chart shown in Figure 11. The computational implementation of the constitutive model proposed in Figure 4 was conducted through the use of the subroutine UMAT, which evaluated the Cauchy stress tensor $\boldsymbol{T}$ and a fourth-order tensor of a tangential stiffness $\boldsymbol{C}$ defined by

$$\boldsymbol{C} = \frac{\partial(d\boldsymbol{T})}{\partial(d\boldsymbol{D})} \tag{18}$$

The ABAQUS/Standard further utilizes a backward-Euler finite difference scheme to update variables. Those variables that are determined from the previous iteration and those that do not change during the iteration between

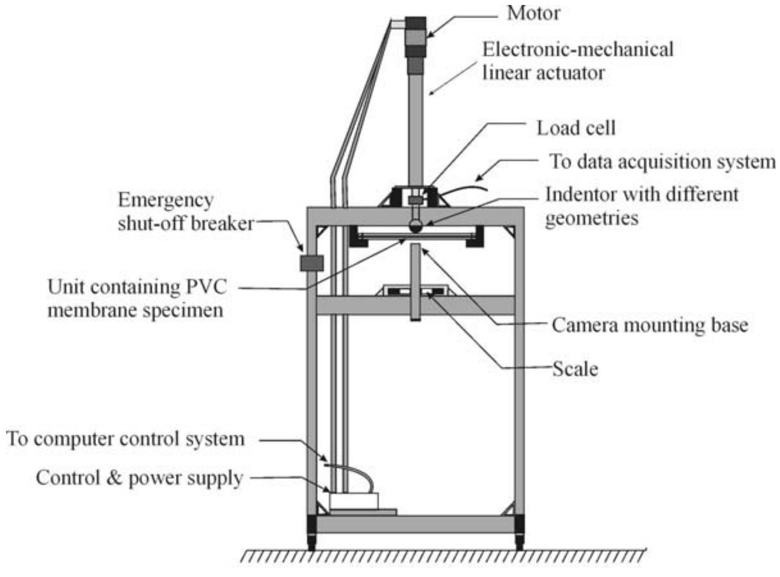

(a) Schematic view of the test frame

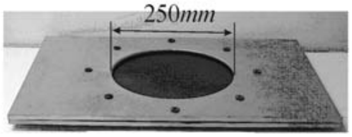

(b) Clamped plate assembly

Figure 7 : Membrane indentation facility

$[t, t+dt]$ can be defined as *state variables*. The *state variables* adopted in the analysis include the components of irreversible deformation gradient $\boldsymbol{F}^u$ and stress tensors in the visco-plastic responses including model A and B, respectively, at time t. The rate-dependent material parameters of the chemically-treated PVC require updated information for $\dot{\gamma}_0$. In previous computations conducted in connection with the modelling of the indentation of an untreated PVC membrane, the field of $\dot{\gamma}_0$ is updated after each iteration during the computation. Such an approach shows extremely slow convergence, when applied to the modelling of the behaviour of the chemically-treated PVC. Especially beyond the yield point, there is an abrupt alteration in the elastic parameter of the sub-model A # of the constitutive model and this gives rise to a slow convergence process. In this study, we first obtain an approximate estimate of the time-history of $\dot{\gamma}_0$ while considering the material to be fully elastic. When the time-history of $\dot{\gamma}_0$ for a particular element is estimated at a number of displacement increments, the value of $\dot{\gamma}_0$ for that element at a particular displacement can be then interpolated. This approach showed stable numerical results and was adopted for the model representations of the uniaxial test data for the chemically-treated PVC material subjected to a 9-*month* exposure to pure ethanol. The modelling was conducted up to failure using the constitutive equations proposed in Table 1 and material parameters given in Table 2. Both a quadratic triangular membrane element 3M6 and a linear solid triangular prism element C3D6 were used in the computational modeling. The results indicated no noticeable differences in the performance of the two types of elements. The computational results shown in Figure 12 were obtained using the solid element, and are the predicted responses at two different peak strains $\varepsilon_0 = 10\%, 60\%$. Although the time history of $\dot{\gamma}_0$ is estimated, the computations show a good correlation with the experimental results. The computational approach is then adopted for the modelling of both the axisymmetric and the asymmetric indentation of the chemically-treated circular membrane.

The geometry of the axisymmetric membrane indentation problem is illustrated in Figure 13a. The bound-

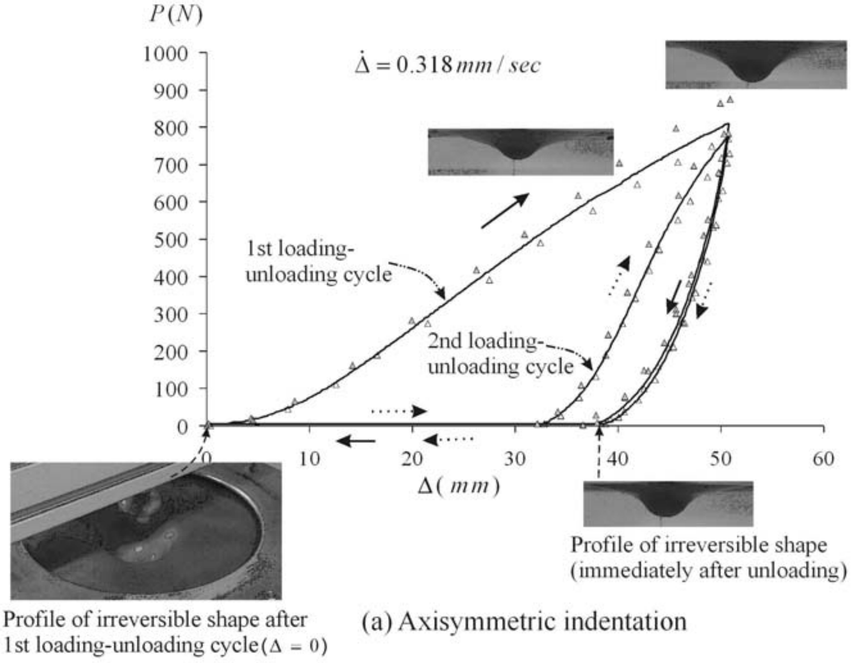

(a) Axisymmetric indentation

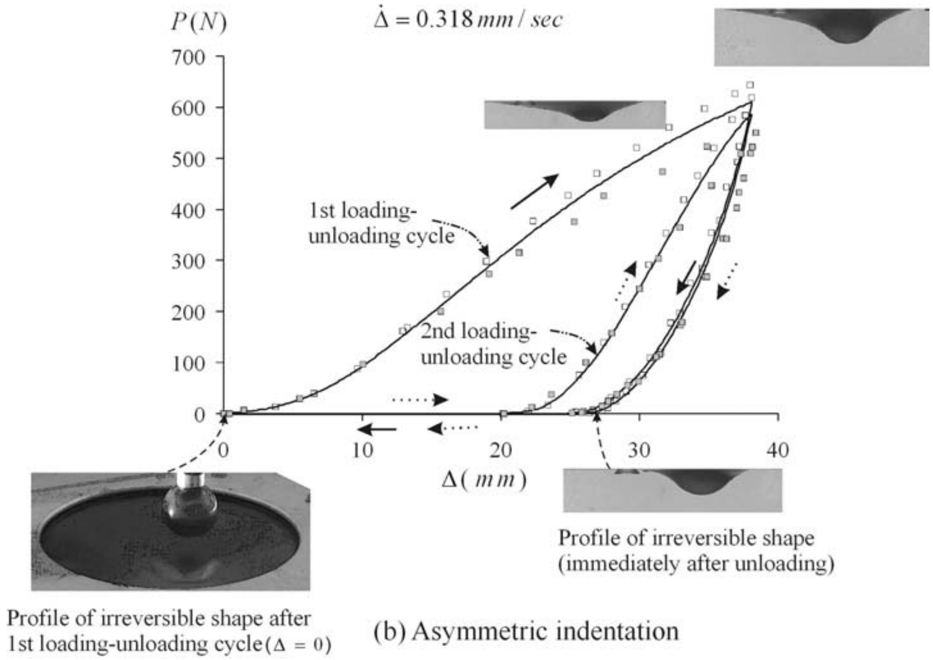

(b) Asymmetric indentation

Figure 8 : Load-displacement responses of the treated PVC membrane exposed to pure ethanol for 9 *months* subjected to axisymmetric indentation and asymmetric indentation (symbols represent experimental scatter)

ary conditions and finite element discretization used in the computational modelling are indicated in Figure 13b. In the axisymmetric indentation problem, a rigid spherical indentor is centrally positioned to move normal to the plane of the edge supported circular membrane. The contact conditions between the indentor and the membrane have been chosen as the standard hard contact option available in the ABAQUS/Standard code. The computational modelling of the axisymmetric indentation is performed for a loading rate of $\dot{\Delta} = 0.318 mm/\text{sec}$. The computation first considers the case where the contact between the indentor and the chemically-treated PVC

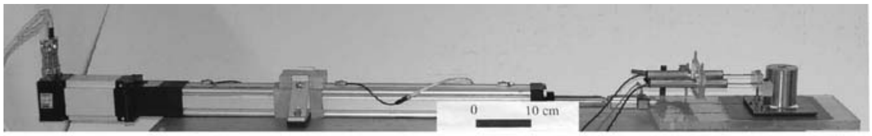

(a) Experimental setup

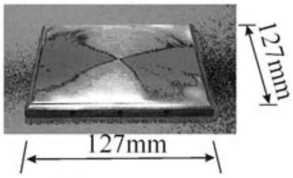

(b) Sliding brass plate

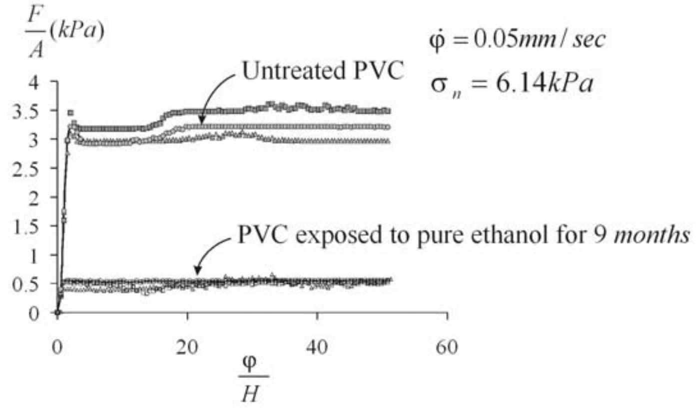

(c) Experimental results (symbols represent experimental scatter)

Figure 9 : Determination of the friction coefficient between a brass plate and PVC (φ: relative displacement between brass plate and PVC membrane; H: thickness of the PVC membrane; F: friction force; A: contact area; σ_n: normal stress at the contact plane)

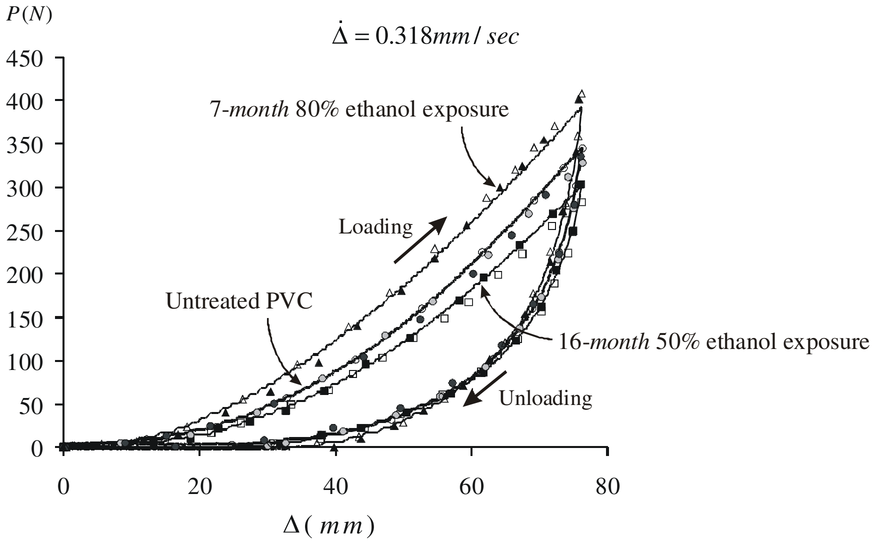

Figure 10 : Load-displacement responses of chemically-treated PVC membrane exposed to lower concentrations of ethanol subjected to axisymmetric indentation (symbols represent experimental scatter)

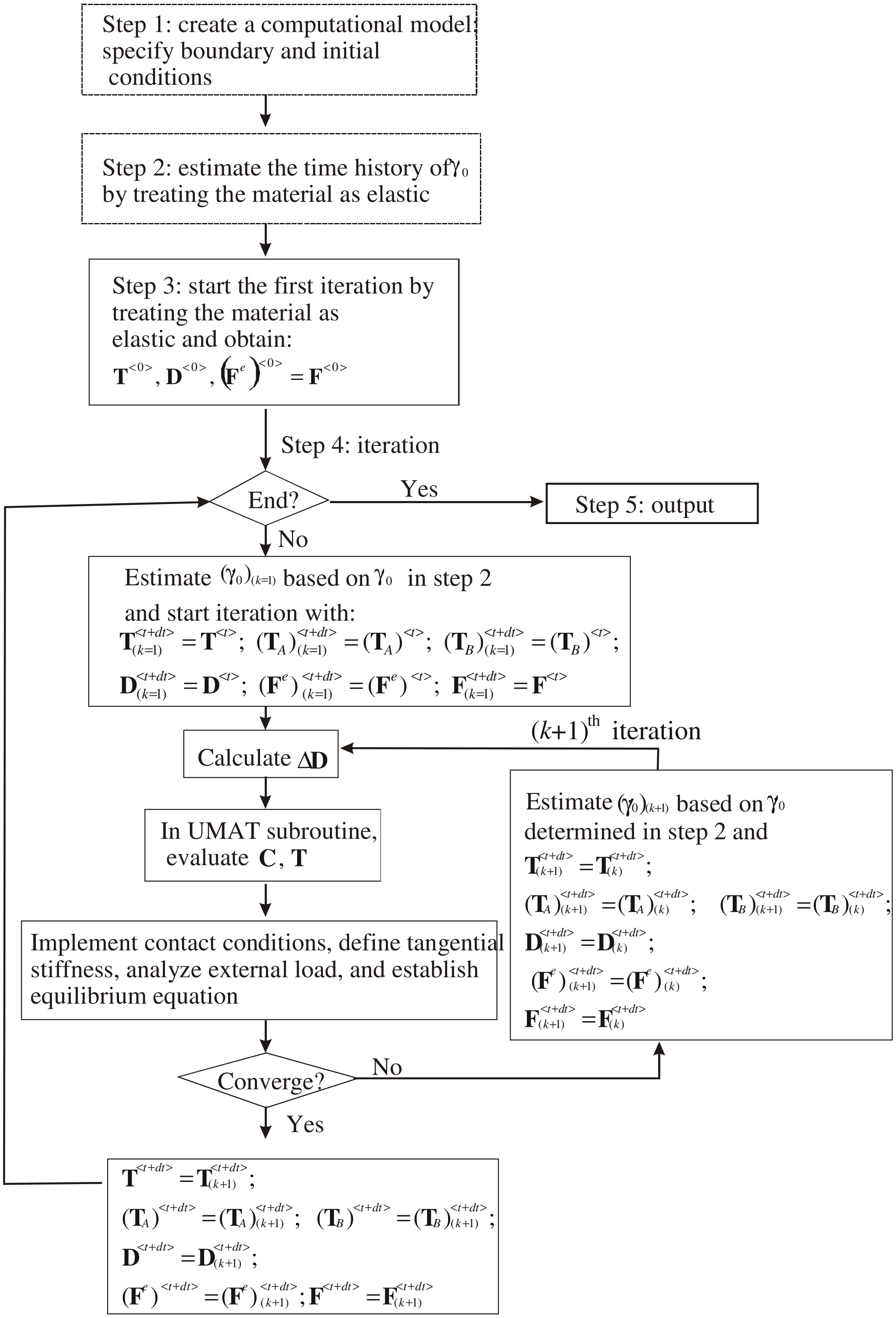

Figure 11 : Computational procedures used in ABAQUS

membrane is frictionless.

Figure 14 shows the comparison of the load-displacement response determined from the computational modelling with equivalent results derived from the axisymmetric indentation with a specified loading rate. For purposes of comparison, results are also presented for the unloading mode. The computations were also carried out to include the case where the friction coefficient was determined from experiment (i.e. $\mu = 0.08$) and the case where friction coefficient was an order of magnitude higher than that determined from experiment (i.e. $\mu = 1.0$). As observed, the computational results at $\mu = 0.08$ tend to match the experimental data more accurately.

The computations also attempt to correlate the predicted deflected shapes with those recorded in the experiments. The computational estimates for the deflected profiles at different loading-unloading stages are presented in Figure 15. The (x,z) coordinates of the deflected profile shown in Figure 8a were determined using an image analysis procedure (Klette, et al., 1998). In this procedure, the physical dimensions of the coordinates, measured in terms of *pixels* in the image plane, can be obtained from a calibration against two scales of known dimensions that are located equidistant from the center of the membrane. The centers of both scales were aligned on a plane whose normal was parallel to the optical axis of the camera. Figure 15a presents results for three indentational displacements $\Delta = 12.7mm$, $25.4mm$ and $50.8mm$ obtained during the loading stage and Figure 15b shows the profile of the deflected shape in the completely unloaded state. Due to the visco-plastic effects in the polymeric material, the membrane experiences irreversible deformations after a complete loading-unloading cycle. As a result, the deflected profiles during loading differ from those determined during the unloading stage. When the indentation displacement Δ reduces to zero after a complete loading-unloading cycle, the membrane exhibits a pronounced permanent deformation. The computational results show an accurate prediction of the deflected profile during the loading stage, whereas the procedure slightly overestimates magnitude of these irreversible deflections. The overestimation of the irreversible deformation is also visible in the load-displacement response shown Figure 14.

We now focus on the problem involving the asymmetric indentation of a chemically-treated polymeric membrane. Figure 16a illustrates the geometry of the membrane, the location of the asymmetric indentation and the boundary conditions. The mesh discretization is shown in Figure 16b. During asymmetric indentation, contact is established at a distance $\Omega = 42mm$ from the center of the circular membrane. The asymmetric indentation is also performed at a loading rate of $\dot{\Delta} = 0.318mm/\text{sec}$. The computations first consider the case involving frictionless contact between the indentor and the chemically-treated PVC membrane (Figure 17). The discrepancy between the experimentally derived load-displacement responses and the computational equivalents is more pronounced for the case involving asymmetric indentation. The asymmetric indentation of the chemically-treated PVC membrane can involve greater relative slip between the indentor and PVC membrane than in the case of axisymmetric indentation. Therefore the influence of the variation in the friction coefficient is more noticeable. Figure 18 presents a comparison between the deflected profiles derived from computational modelling and experimental results for the case involving a friction coefficient $\mu = 0.08$. The results are presented for three indentation displacements $\Delta = 25.4mm$, $31.8mm$ and $38.1mm$. As with the situation involving axisymmetric indentation, the computations provide an accurate representation for the deflected profiles during the loading stage, whereas the modelling slightly overestimates the irreversible deformation during complete unloading of the membrane. The overestimation of the irreversible deformation is also evident in the load-displacement response presented in Figure 17.

5 Conclusions

The mechanical behaviour of a PVC membrane subjected to various levels of exposure to ethanol was examined via an indentation test. The experimental research examines the problem of a chemically-treated flat circular PVC membrane that is fixed at its boundary and subjected to both axisymmetric and asymmetric indentation. The indentation problem provides a useful technique for assessing the loss of the flexibility of the PVC material subjected to various levels of exposure to ethanol. The response of the PVC membrane subjected to pure ethanol exposure indicates a stiffness increase and a loss of flexibility and these effects diminish as the level of concentration decreases. In particular, a constitutive model, which incorporates yield-type phenomena, large strain deformability, irreversible effects and strain-rate sensitiv-

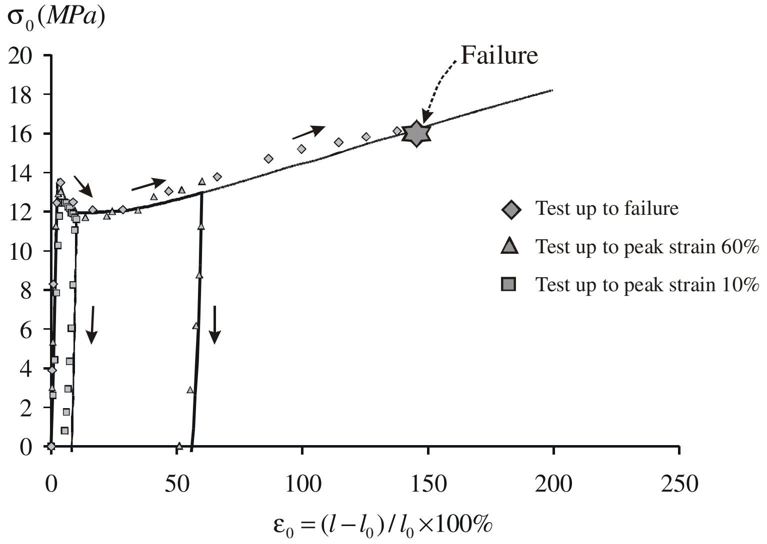

(a) $\dot{\varepsilon}_0 = 4\%/min$

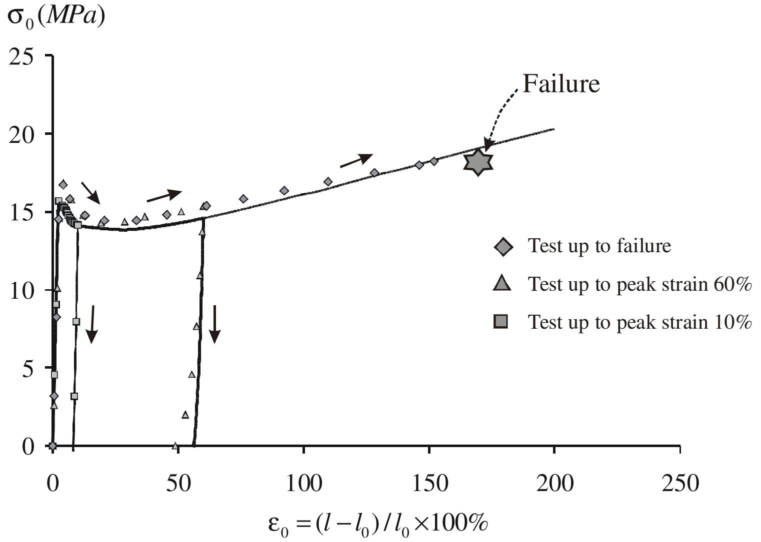

(b) $\dot{\varepsilon}_0 = 40\%/min$

Figure 12 : Model representation by ABAQUS software of the stress-strain responses involving loading and unloading of treated PVC exposed to pure ethanol for 9 *months*

ity, is proposed for describing the mechanical behaviour of a PVC membrane subjected to a 9-*month* exposure to pure ethanol. The material parameters determined through the uniaxial tensile testing have been used to characterize the constitutive behaviour of the chemically-treated PVC. The constitutive model is implemented in a computational code to predict the response of the membrane indentation tests. The results show that the computations can reasonably duplicate the trends in the experimental responses for the cases involving axisymmetric and asymmetric indentation of the clamped circular membrane. The deflected shapes predicted from the computational approach correlate well with the experimental data particularly in the loading stage. An overestimation of the irreversible deformation is observed during the unloading stage.

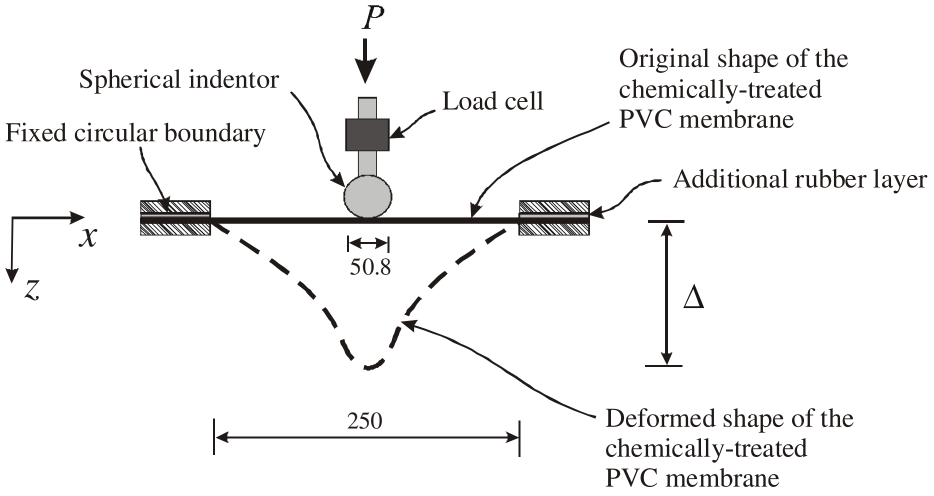

(a) Axisymmetric indentation (all dimensions in *mm*)

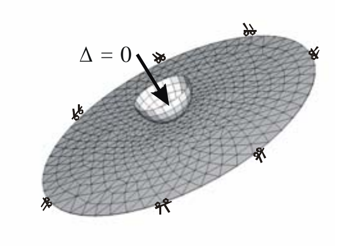

(b) Mesh configurations and boundary conditions
(Total number of elements: 862)

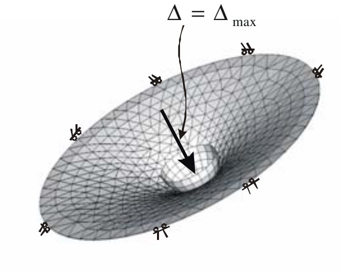

(c) Deformed shape during maximum indentation

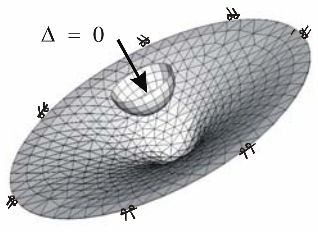

(d) Irreversible shape after a loading-unloading cycle

Figure 13 : Computational results of axisymmetric indentation on a chemically-treated PVC membrane.

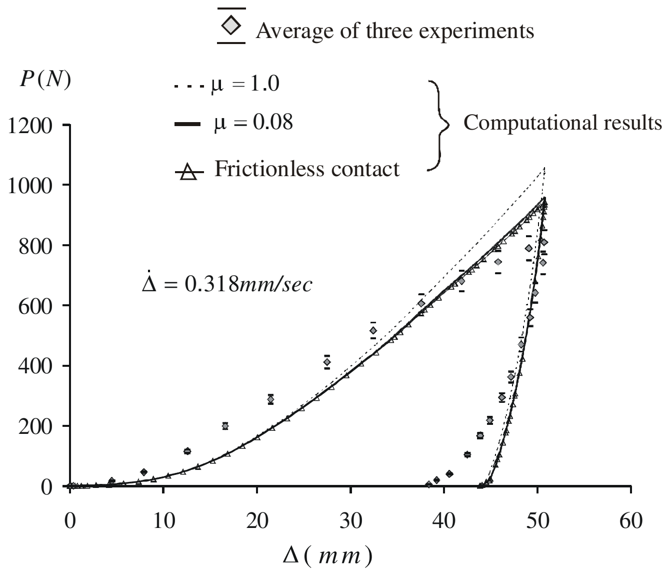

Figure 14 : Load-displacement responses of the chemically-treated PVC membrane subjected to axisymmetric indentation (symbols represent experimental data).

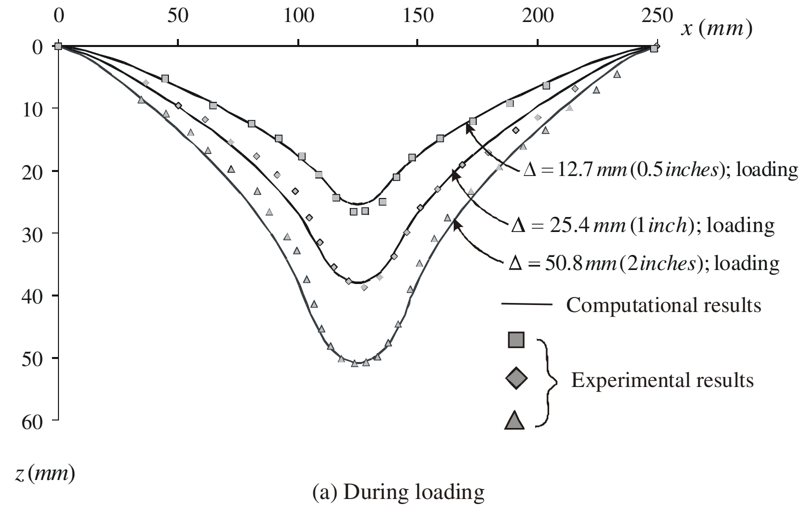

(a) During loading

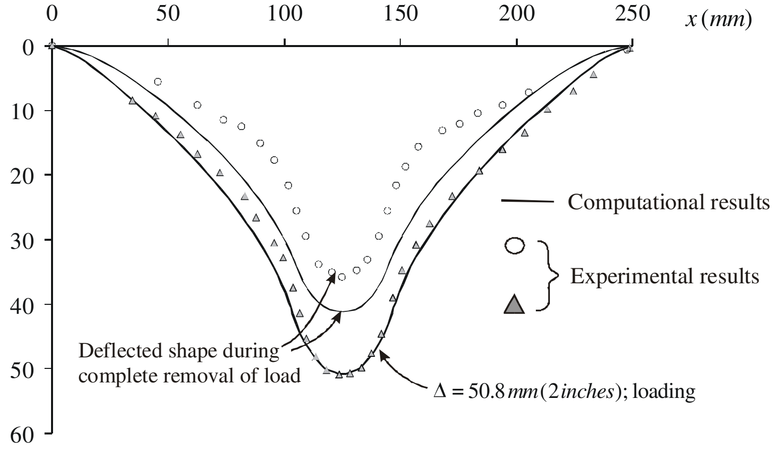

(b) During unloading

Figure 15 : Deflected shapes of a chemically-treated PVC membrane during axisymmetric indentation ($\mu = 0.08$; $\dot{\Delta} = 0.318\,mm/\text{sec}$; symbols represent experimental data)

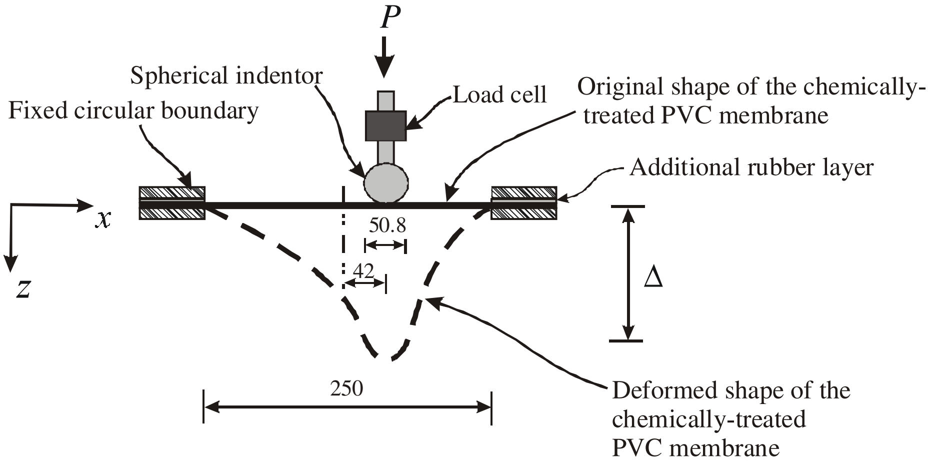

(a) Asymmetric indentation (dimensions in *mm*)

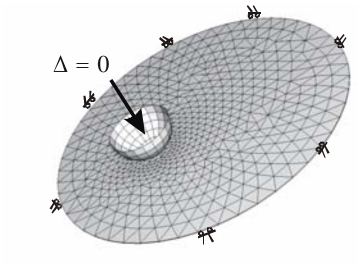

(b) Mesh configurations and boundary conditions (Total number of elements: 1198)

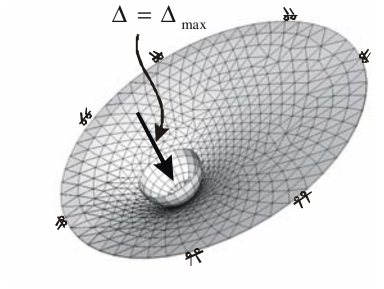

(c) Deformed shape during maximum indentation

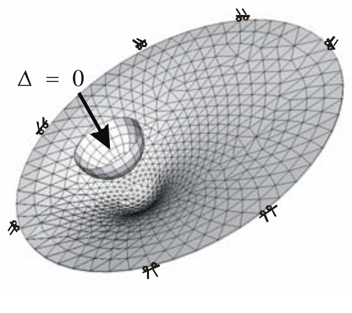

(d) Irreversible shape after a loading-unloadingt cycle

Figure 16 : Computational results of axisymmetric indentation on a chemically-treated PVC membrane

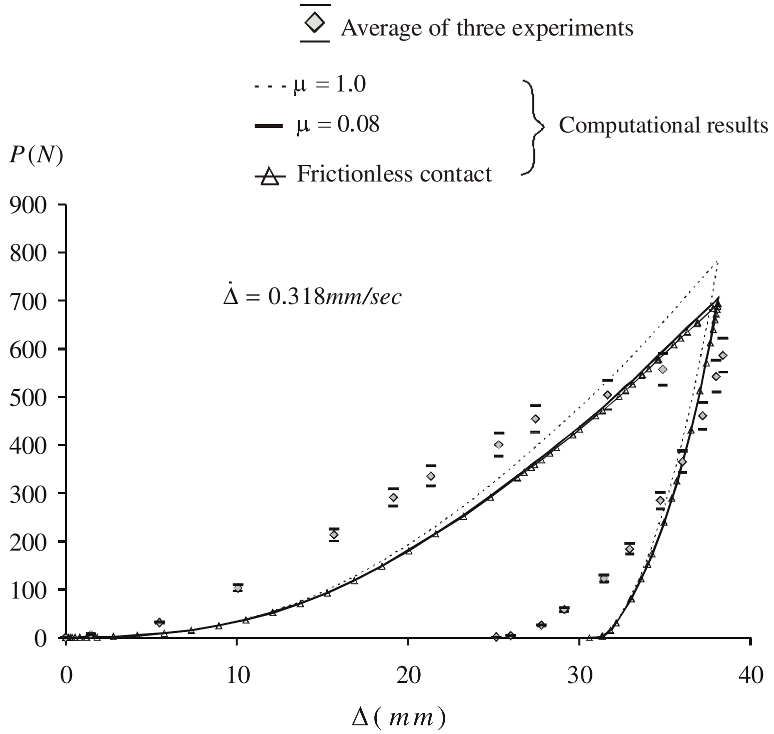

Figure 17 : Load-displacement responses of the chemically-treated PVC membrane subjected to asymmetric indentation (symbols represent experimental data)

Acknowledgement: The work described in the paper was supported through a *Discovery Grant* awarded by the Natural Sciences and Engineering Research Council of Canada to the first author, who would also like to acknowledge the research support received by the Max Planck Gesellschaft through the Award of the *2003 Max Planck Forschungspreis in the Engineering Sciences*. The first author would also like to thank Professor Dr. Lothar Gaul and colleagues at the Institut A für Mechanik, Universität Stuttgart for their hospitality during visits, which enabled the preparation of the paper.

References:

ABAQUS/Standard (2004): *A General-Purpose Finite Element Program*, Hibbitt, Karlsson & Sorensen, Inc., Pawtucket, RI, USA.

Ahzi, S.; Makradi, A.; Gregory, R.V.; Edie, D.D. (2003): Modeling of deformation behavior and strain-induced crystallization in poly(ethylene terephthalate) above the glass transition temperature. *Mech. Mat.*, vol. 35, pp. 1139-1148.

Aiken, W.; Alfrey, T.; Janseen, A.; Mark, H. (1947): Creep behavior of a plasticized vinylite VYNW. *J. Polym. Sci.*, vol. 2, pp. 178-198.

Alfrey, T.; Wiederhorn, N.; Stein, R.; Tobolsky, A. (1949a). Plasticized polyvinyl chloride: structure and mechanical behaviour. *Indust. Eng. Chem.*, vol. 41, pp. 701-703.

Alfrey, T; Wiederhorn, N.; Stein, R.; Tobolsky, A. (1949b): Some studies of plasticized polyvinyl chloride. *J. Colloid. Sci.*, vol. 4, pp. 211-227.

Arruda, E.M.; Boyce, M.C.; Jayachandran, R. (1995): Effects of strain rate, temperature and thermomechanical coupling on the finite strain deformation of glassy polymers. *Mech. Mat.*, vol. 19, pp. 193-212.

Bacaloglu, R.; Fisch, M. (1995): Degradation and stabilization of poly (vinyl chloride). V. Reaction mechanism of poly(vinyl chloride) degradation. *Polym. Degrad. Stab.*, vol. 47, pp. 33-57.

Beatty, M.F. (1987): Topics in finite elasticity: hyperelasticity of rubber, elastomers, and biological tissues-with examples. *Appl. Mech. Rev.*, vol. 40, pp. 1699-1734.

Bishop, S.; Isaac, D.H.; Hinksman, P.; Morrissey, P. (2000): Environmental stress cracking of poly(vinyl

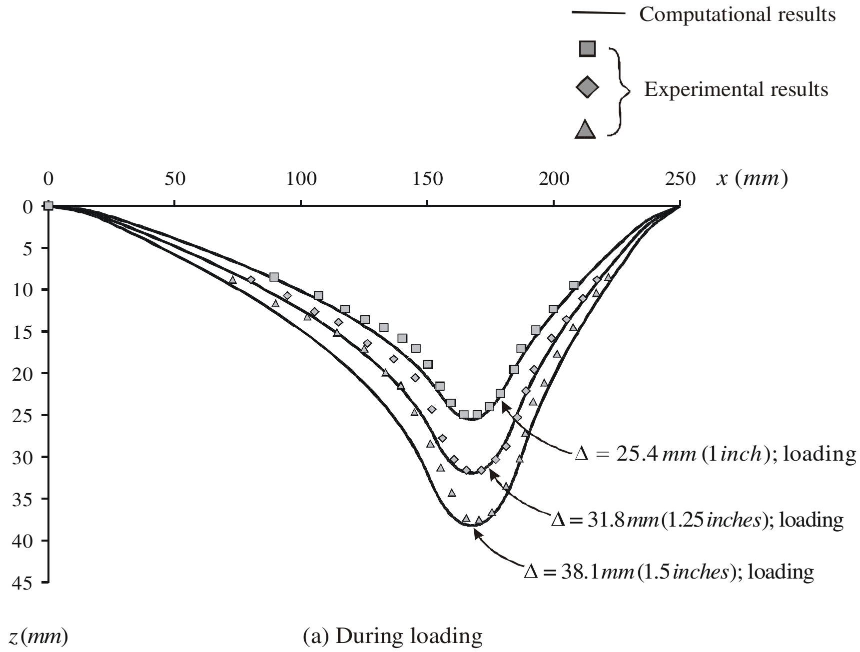

(a) During loading

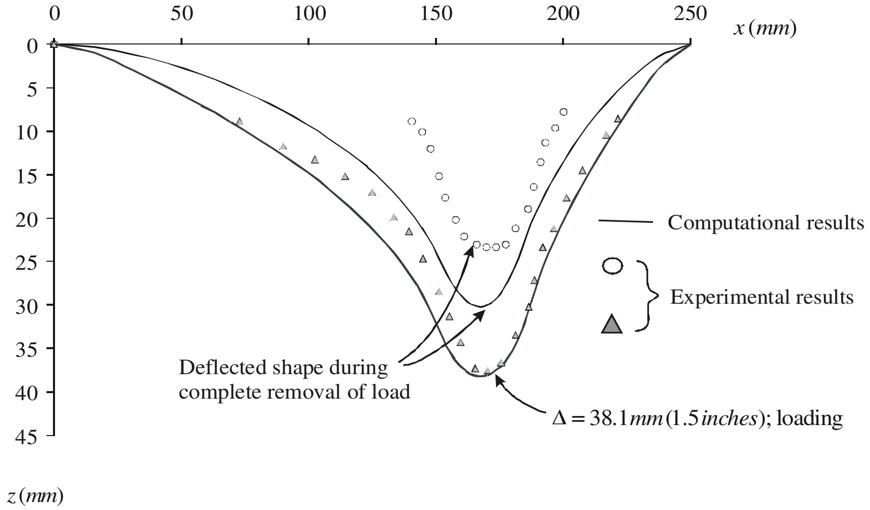

(b) During unloading

Figure 18 : Computational results of axisymmetric indentation on a chemically-treated PVC membrane ($\mu = 0.08$; $\dot{\Delta} = 0.318\,mm/\text{sec}$; symbols represent experimental data)

chloride) in alkaline solutions. *Polym. Degrad. Stab.*, vol. 70, pp. 477-484.

Boue, F.; Edwards, S.F.; Vilgis, T.A. (1988): The entropy of a network of rod molecules. *J. Phys.*, vol. 49, pp. 1635-1645.

Boyce, M.C.; Parks, D.M.; Argon, A.S. (1988a): Large inelastic deformation of glassy polymers, part I: rate dependent constitutive model. *Mech. Mat.*, vol. 7, pp. 15-33.

Boyce, M.C.; Parks, D.M.; Argon, A.S. (1988b): Large inelastic deformation of glassy polymers. Part II: numerical simulation of hydrostatic extrusion. *Mech. Mat.*, vol. 7, pp. 35-47.

Cazzuffi, D.; Fede, L.; Villa, C.; Montanelli, F.; Rimoldi, P. (1995): The assessment of the effects of natural and lab weathering exposure of geosynthetics. In: *Proceedings Sardinia 95, Fifth International Landfill Symposium*, pp. 387-396.

Clifton, R.J. (1972): On the equivalence of $\boldsymbol{F}^e\boldsymbol{F}^p$ and $\boldsymbol{F}^p\boldsymbol{F}^e$. *J. Appl. Mech., Trans. ASME*, vol. 39, pp. 287-289.

Contamin, B.; Debeauvais, V. (1998): *The Effect of Ethanol Exposure on Burst Strength of a Geomembrane*, Research Report, McGill University.

Diebel, P. (2002): Formulation, manufacturing and physical properties of PVC geomembranes. In: *PVC Geomembrane Institute Technology Program: Constructing with PVC Geomembrane: Video Series, Lecture 1, PVC Geomembrane Institute*, University of Illinois at Urbana-Champaign.

Dorfmann, A.; Ogden, R.W. (2004): A constitutive model for the Mullins effect with permanent set in particle-reinforced rubber. *Int. J. Solids Struct.*, vol. 41, pp. 1855-1878.

Edwards, S.F. (1971): Statistical mechanics of rubber. In: Chompff, A.J., Newman, S., (ed.), *Polymer Networks: Structural and Mechanical Properties*, Plenum Press, New York, pp. 83-110.

Farris, R.J. (1971): The stress-strain behaviour of mechanically degradable polymers. In: Chompff, A.J. and Newman, S., (ed.), *Polymer Networks: Structural and Mechanical Properties*, Plenum Press, New York, pp. 341-392.

Flory, P.J. (1969): *Statistical Mechanics of Chain Molecules*, Wiley Interscience, New York.

Green, A.E.; Adkins, J.E. (1970): *Large Elastic Deformations*, Oxford University Press, London.

Gurtin, M.E.; Anand, L. (2005): The decomposition $\boldsymbol{F} = \boldsymbol{F}^e\boldsymbol{F}^p$, material symmetry, and plastic irrotationality for solids that are isotropic-viscoplastic or amorphous. *Int. J. Plast.*, vol. 21, pp. 1686-1719.

Haedrich, T. (1995): *The Effect of Chemical Exposure on the Burst Strength of a Geomembrane*, M.Eng., Thesis, Carleton University, Ottawa.

Haxo, H.E.; Haxo, P.D. (1989): Environmental conditions encountered by geosynthetics in waste containment applications. In: Koerner, R.M., (ed.), *Durability and Aging of Geosynthetics*, Elsevier, London and New York.

Jones, J.L.; Marques, C.M. (1990): Rigid polymer network models. *J. Phys.*, vol. 51, pp. 1113–1127.

Khalifa, B.A.; Morsi, S.E.; Khalifa, W.M.; Barsoum, S. (1979): The effect of ultraviolet radiation on the physical properties of stabilized poly(vinyl chloride), *Br. Polym. J.*, vol. 24, pp. 13-16.

Klette, R.; Karsten, S.; Andreas, K. (1998): *Computer vision: Three Dimensional Data From Images*, Springer-Verlag, Singapore.

Koerner, E.M. (1994): *Designing with Geosynthetics*, 3^{rd} Ed., Prentice Hall, Upper Saddle River, New Jersey.

Kröner, E. (1960): Allgemeine Kontinuumstheorie der Versetzungen und Eigenspannungen. *Arch. Ration. Mech. Anal.*, vol. 4, pp. 273–334.

Lee, E.H. (1969): Elastic-plastic deformation at finite strains. *J. Appl. Mech.*, vol. 36, pp. 1-6.

Lubarda, V.A. (2004): Constitutive theories based on the multiplicative decomposition of deformation gradient: thermoelasticity, elastoplasticity, and biomechanics. *Appl. Mech. Rev.*, vol. 57, pp. 95-108.

Madorsky, S.L. (1964): *Thermal Degradation of Organic Polymers*, Interscience, New York.

Malvern, L.E. (1969): *Introduction to the Mechanics of a Continuous Medium*, Prentice-Hall, Upper Saddle River.

Masada, T.; Mitchell, G.F.; Sargand, S.M.; Shashikumar, B. (1994): Modified direct shear study of clay liner-geomembrane interfaces exposed to landfill leachate. *Geotext. and Geomembr.*, vol. 13, pp. 165-179.

Matthews, R.G.; Duckett, R.A.; Ward, I.M.; Jones, D.P. (1997): The biaxial drawing behaviour of poly(ethylene terephthalate). *Polymer*, vol. 19, pp. 4795-4802.

Messadi, D.; Vergnaud, J.M.; Hivert, M. (1981): A new approach to the study of plasticizer migration from PVC into methanol. *J. Appl. Polym. Sci.*, vol. 26, pp. 667-677.

Messadi, D.; Vergnaud, J.M. (1982): Plasticizer transfer from plasticized PVC into ethanol-water mixtures. *J. Appl. Polym. Sci.*, vol. 27, pp. 3945-3955.

Mooney, M. (1940): A theory of large elastic deformation. *J. Appl. Phys.*, vol. 11, pp. 583-593.

Mullins, L. (1947): Effect of stretching on the properties of rubber. *J. Rubber Res.*, vol. 16, pp. 275-289.

Mullins, L. (1969): Softening of rubber by deformation. *Rubber Chem. Technol.*, vol. 42, pp. 339-362.

Ogden, R.W. (1984): *Non-Linear Elastic Deformations*, Ellis-Horwood, Chichester.

Owen, D.R. (1970): A mechanical theory of materials with elastic range. *Arch. Rat. Mech. Analysis*, vol. 37, pp. 85-110.

Pereda, J.J.; Aravas, N.; Bassani, J.L. (1993): Finite deformations of anisotropic polymers. *Mech. Mat.*, vol. 15, pp. 3-20.

Pipkin, A.C.; Rivlin, R.S. (1970): Mechanics of rate-independent materials. *J. Appl. Math. Phys. (ZAMP)*, vol. 16, pp. 313-327.

Pita V.J.R.R.; Sampaio, E.E.M.; Monteiro, E.E.C. (2002): Mechanical properties evaluation of PVC/plasticizers and PVC/thermoplastic polyurethane blends from extrusion processing. *Polym. Test*, vol. 21, pp. 545-550.

Pooley, C.M.; Tabor, D. (1972): Friction and molecular structure: the behaviour of some thermoplastics. *Proc. Roy. Soc.*, vol. A329, pp. 251-274.

Qi, H.J.; Boyce, M.C. (2005): Stress-strain behavior of thermoplastic polyurethanes. *Mech. Mat.*, vol. 37, pp. 817-839.

Qian, X.; Koerner, R.M.; Gray, D.H. (2002): *Geotechnical Aspects of Landfill Design and Construction*, Prentice-Hall, Upper Saddle River, New Jersey.

Rittel, D. (1999): On the conversion of plastic work to heat during high strain rate deformation of glassy polymers. *Mech. Mat.*, vol. 31, pp. 131-139.

Rittel, D. (2000): An investigation of the heat generated during cyclic loading of two glassy polymers. Part I: experimental. *Mech. Mat.*, vol. 32, pp. 131-147.

Rivlin, R.S. (1948): Large elastic deformations of isotropic materials. IV. Further developments of the general theory. *Phil. Trans. Roy. Soc.*, vol. A 241, pp. 379-397.

Rivlin, R.S. (1960): Some topics in finite elasticity. In: Goodier, J.N. and Hoff, J.N. (ed), *Structural Mechanics: Proc. 1st Symp. Naval Struct. Mech.*, Pergamon Press, pp. 169-198.

Selvadurai, A.P.S. (2002): Second-order elasticity for axisymmetric torsion: a spheroidal coordinate formulation. In: Croitoro, E., (ed), *Proc. 2nd Canadian Conf. on Nonlinear Solid Mechanics*, Vancouver, vol. 1, pp. 27-49

Selvadurai, A.P.S.; Yu, Q. (2005a) : Constitutive modelling of a polymeric material subjected to chemical exposure, *Int. J. Plast.* (accepted)

Selvadurai, A.P.S.; Yu, Q. (2005b) : On the indentation of a polymeric membrane (submitted)

Septanika, E.G.; Ernst, L.J. (1998a): Application of the network alteration theory for modeling the time-dependent constitutive behaviour of rubbers. Part I. General theory. *Mech. Mat.*, vol. 30, pp. 253-263.

Septanika, E.G.; Ernst, L.J. (1998b): Application of the network alteration theory for modeling the time-dependent constitutive behaviour of rubbers. Part II. Further evaluation of the general theory and experimental verification. *Mech. Mat.*, vol. 30, pp. 265-273.

Shin, S.M.; Jeon, H.S.; Kim, Y.H.; Yoshioka, T.; Okuwaki, A. (2002): Plasticizer leaching from flexible PVC in low temperature caustic solution. *Polym. Degrad. Stab.*, vol. 78, pp. 511-517.

Spencer, A.J.M. (1970): The static theory of finite elasticity. *J. Inst. Math. Appl.*, vol. 6, pp. 164-200.

Spencer, A.J.M. (2004): *Continuum Mechanics*, 3rd Ed., Dover Publ., London.

Sweeney, J.; Ward, I.M. (1995): Rate dependent and network phenomena in the multiaxial drawing of poly(vinyl chloride). *Polymer*, vol. 36, pp. 299-308.

Treloar, L.R.G. (1943): Stress-strain date for vulcanized rubber under various types of deformation. *Trans. Faraday Soc.*, vol. 39, pp. 59-70.

Treloar, L.R.G. (1975): *Rubber Elasticity*, 3rd Ed., Oxford University Press, London.

Yu, Q.; Selvadurai, A.P.S. (2005): Mechanical behaviour of a plasticized PVC subjected to ethanol exposure. *Polym. Degrad. Stab.*, vol. 89, pp. 109-124.